Clays and Clay Minerals, Vol. 48, No. 2, 282–289, 2000.

MIXED LAYERING OF ILLITE-SMECTITE: RESULTS FROM HIGH-RESOLUTION TRANSMISSION ELECTRON MICROSCOPY AND LATTICE-ENERGY CALCULATIONS

JUAN OLIVES, MARC AMOURIC, AND RÉGIS PERBOST

CRMC2-CNRS, Campus de Luminy, Case 913, 13288 Marseille cedex 09, France

Abstract—Mixed layering of illite-smectite was studied both experimentally, by using high-resolution transmission electron microscopy (HRTEM) and analytical electron microscopy (AEM), and theoretically, by using lattice-energy calculations.

Samples from a hydrothermal origin show the transformation of smectite to illite with different ordering types in the illite-smectite layer sequences. Ordering ranges from complete disordered (Reichweite, R = 0 type) in the less transformed samples to increased local order, with IS and IIS sequences (R = 1 and R = 2, respectively; I = illite, S = smectite) in more illitized samples.

Lattice-energy calculations are used to determine the structure of the illite-smectite sequence, which corresponds to the minimum energy. The unit layers are: $O_{0.5}TI'TO_{0.5}$ (O, T, and I', respectively, denote the octahedral and tetrahedral sheets, and the interlayer. The 0.5 signifies half of the octahedral cations.) For example, the arrangements of the perfectly ordered . . . ISIS . . . and . . . IISIIS . . . sequences are respectively . . . $O_M(TI'T)_IO_M(TI'T)_S$ . . . and . . . $O_M(TI'T)_IO_I(TI'T)_IO_M(TI'T)_S$ . . . (the subscripts I, S, and M, respectively, refer to compositions of illite, smectite, and midway between at 0.5). Such arrangements produce a polar model for TOT layers, which display a $T_IO_MT_S$ structure in the case of IS adjacent layers. Furthermore, the lattice energies of . . . ISIS . . . and . . . IISIIS . . . are found to be nearly equal to the corresponding sums of the lattice energies of illite and smectite. This result indicates that interstratified illite-smectite and the two-phase assemblage of illite + smectite have similar stabilities.

On the basis of the above model, the solid-state transformation of one smectite layer to one illite layer, which produces mixed-layer sequences, involves the transformation of an $O_{0.5}TI'TO_{0.5}$ unit of smectite into the same corresponding unit of illite.

Key Words—HRTEM-AEM, Illite-Smectite, Lattice-Energy Calculations, Mixed Layering, Polar 2:1 Layers.

INTRODUCTION

The transformation of smectite to illite is a reaction which occurs during diagenesis or at hydrothermal conditions. Mixed layering of illite-smectite, which results from this process, has been intensively studied by X-ray diffraction (XRD; *e.g.*, Środoń, 1984; Inoue *et al.*, 1987; Reynolds, 1992) and directly observed by high-resolution transmission electron microscopy (HRTEM). According to computer-image simulations of Guthrie and Veblen (1989, 1990), illite and smectite layers can be commonly differentiated by using microscope overfocus conditions. On such a basis, sequences of illite-smectite interstratification of either disordered or ordered types, were observed by HRTEM (*e.g.*, Ahn and Peacor, 1989; Veblen *et al.*, 1990; Jiang *et al.*, 1990; Amouric and Olives, 1991; Murakami *et al.*, 1993; Olives and Amouric, 1994a, 1994b; Huggett, 1995). Information about illitization mechanisms (solid-state, dissolution-crystallization) was also obtained from HRTEM observations (Amouric and Olives, 1991; Buatier *et al.*, 1992; Murakami *et al.*, 1993).

Amouric and Olives (1991) presented HRTEM observations on illite, smectite, and illite-smectite (involving hydrated smectite with $d(001)$ = 1.25 nm) in a smectite-rich sample from hydrothermal origin and showing a smectite-to-illite transformation. The present paper completes this study with two additional illitic samples. These three samples are representative of this hydrothermal transformation and show various (disordered and ordered) illite-smectite interstratification sequences as observed by HRTEM. In addition, the chemical variations of the mixed-layer minerals are characterized by analytical electron microscopy (AEM).

A theoretical approach on the basis of lattice-energy calculations is used to determine the structure of mixed-layer illite-smectite by energy minimization methods. The approach considers various types of polar and non-polar 2:1 layers (see Olives and Amouric, 1994a, 1994b). Energy calculations also lead to a better understanding of the relative stability of these minerals and yield a description at the unit-cell scale of the solid-state illitization mechanism.

MATERIALS AND METHODS

The studied materials belong to a hydrothermal series from the Shinzan area, Akita Prefecture, Japan. In this area, the hydrothermal alteration of silicic volcanic glass (Miocene Epoch) produced a series between smectite and illite. The mineral assemblage consists of interstratified illite-smectite, illite, smectite, quartz,

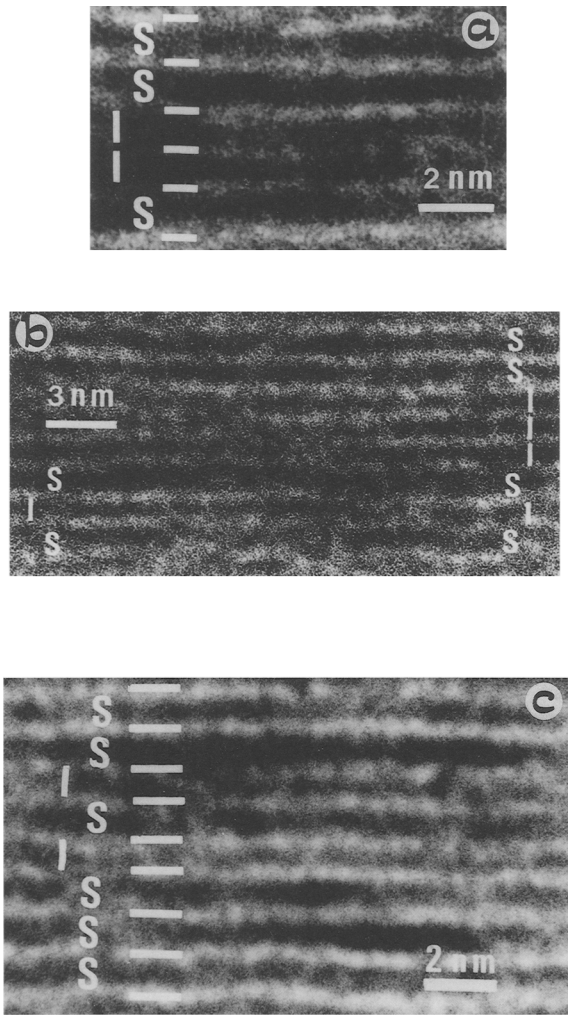

Figure 1. Lattice-fringe images of various randomly disordered mixed-layer illite-smectite sequences, from the smectite-rich sample studied here (see text). [Image (a) from Amouric and Olives, 1991, and (b) from Olives and Amouric, 1994a.]

and chlorite (Inoue and Utada, 1983). The three specimens selected contain interstratified illite-smectite with, respectively, 68, 40, and 20% smectite, as determined by XRD (Inoue *et al.*, 1987).

The samples, reduced to a powder and embedded in Araldite resin, were cut with a diamond knife of an LKB Ultramicrotome. The <50-nm thick sections were deposited on carbon-coated copper grids. This technique better preserves smectite from dehydration than ion milling. Bright-field images were taken with a JEOL 2000 FX electron microscope (200-kV accelerating voltage, 1.8-mm spherical aberration coefficient) with a 50-μm objective aperture. Focus values were in the range +50 to +100 nm for one-dimensional images and of about −100 nm for two-dimensional images. Specimens were observed at very low beam intensity with a low-light camera to reduce possible damage caused by the electron beam. The microscope is equipped with a Tracor (TN 5502) energy-dispersive X-ray spectrometer using a Si(Li) detector for AEM. Chemical microanalyses were obtained using a beam diameter of 5–20 nm at a constant beam current. Data were processed by a program based on the method of Cliff and Lorimer (1975). Note that possible volatility of elements is accounted for by this method, because the elemental constituents are obtained by comparison to appropriate layer-silicate standards.

EXPERIMENTAL RESULTS

In the smectite-rich sample, three minerals coexist: smectite, illite, and interstratified illite-smectite. In the other samples, only illite and interstratified illite-smectite were present. Owing to the experimental techniques used (ultramicrotome cutting, low electron-beam intensity), the smectite crystallites showed $d(001)$ values of 1.25 nm, indicating that H_2O was present in the interlayer (Amouric and Olives, 1991). This observation was used to identify 1-nm repeat distances as illite (and 1.25-nm repeats as smectite). In images of interlayered minerals, the positions of the lattice fringes are sensitive to experimental conditions (*e.g.*, focus, crystal orientation, crystal thickness). The simulations of Guthrie and Veblen (1990) showed that, under special conditions (overfocus), bright lattice fringes may overlay the octahedral sites of the 2:1 layer, thus leading to a close correspondence between the spacings of the bright lattice fringes and layer thickness. Images of mixed-layer illite-smectite (Figures 1 and 2) were obtained with such conditions. Representative examples of these images are presented in Figure 2a and 2c which shows two sets of fringes: (1) dark fringes of 1.25-nm thickness and (2) gray fringes of 1-nm thickness, which correspond to smectite and illite layers, respectively.

Mixed-layer illite-smectite

In the smectite-rich sample, the observed sequences of illite-smectite interstratification are disordered (Amouric and Olives, 1991). For example, Figure 1 shows the respective interlayering sequences SIISS, SISIIISS, and SSSISISS (S = smectite, I = illite). We consider the sequences as alternations of packets of smectite units and packets of illite units, with the respective numbers of units of N_S and N_I, where N_S and N_I are integers. In general, the sequences of this sample may be described as randomly disordered interstratifications (Reichweite, R = 0) in which N_S and N_I are equal to 1–5 and 1–3, respectively.

Because no significant differences were found in the interlayering sequences between the more illitic samples, they are referred to as illite-rich samples. In these samples, consecutive smectite layers were not ob-

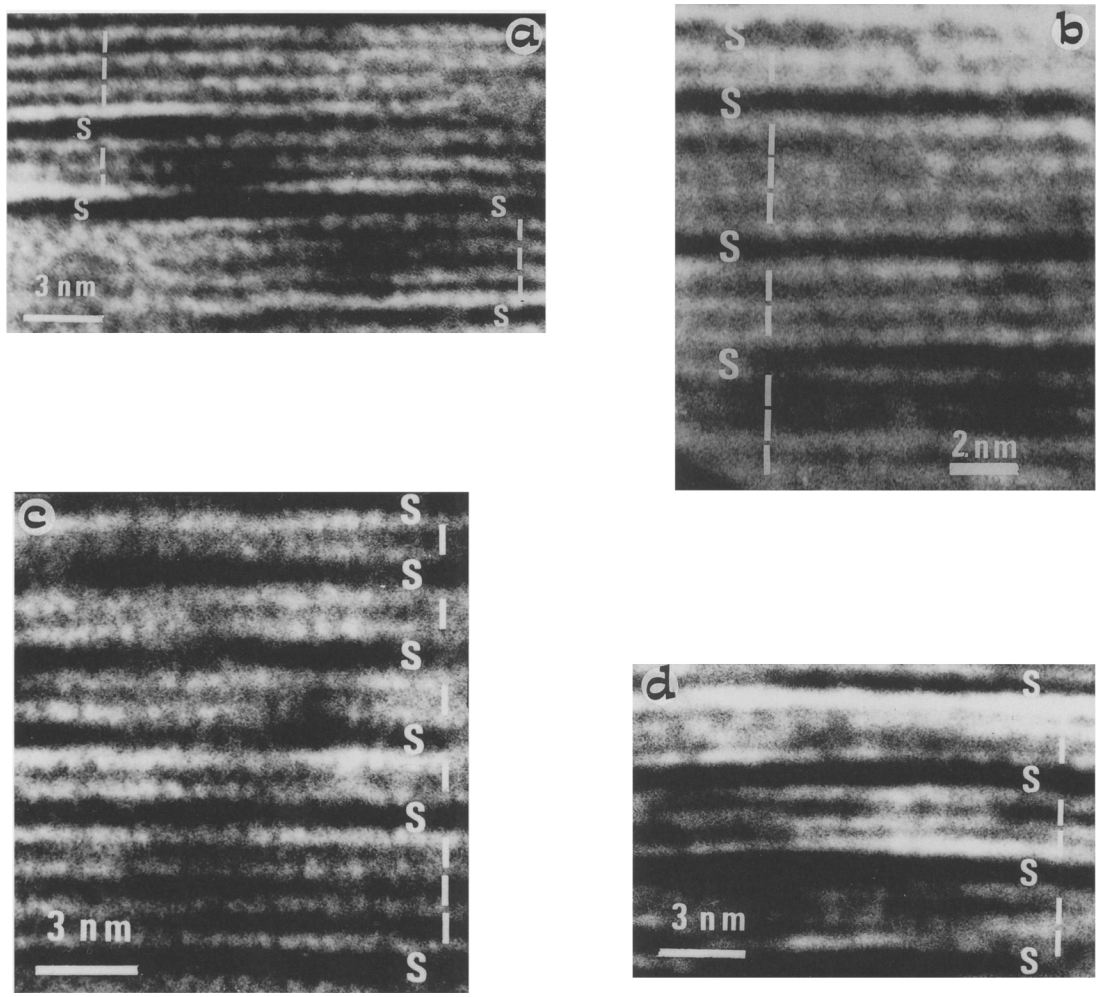

Figure 2. Lattice-fringe images of various locally ordered mixed-layer illite-smectite sequences, from the illite-rich samples studied here (see text). Note perfect R = 1 order in (c), and R = 2 in (d). [Images (a), (c), and (d) from Olives and Amouric, 1994a.]

served, which clearly indicates an ordered interstratification, *i.e.*, R ≥ 1. Such interstratifications are illustrated in Figure 2a and 2b by SIIISIISIII and IIISI-ISIIISIS. Thus, such sequences are described with N_S = 1 and N_I varying from 1 to 3. Locally, perfectly ordered R = 1 sequences (ISIS . . .) or R = 2 sequences (IISIIS . . .) were observed also, involving a few repeat units: *e.g.*, four consecutive IS units in Figure 2c, and three IIS units in Figure 2d. Such a trend, from disordered interstratification sequences to locally ordered sequences, as the percentage of smectite decreases, is similar to the case of interstratified kaolinite-smectite (Amouric and Olives, 1998).

Illite

No significant change was observed in the morphology and the polytypism of illite crystals among the three samples. The previous descriptions (Amouric and Olives, 1991) remain valid for all the samples. Illite crystals contain 7–20 parallel layers and have a lateral extension of 50–200 nm. In two-dimensional structure images, each interlayer region appears as a line of white dots with 0.45-nm spacing, and the shift between two consecutive such lines represents the projected stagger between the two tetrahedral sheets T of the (2:1) TOT layer, where O represents the octahedral sheet of the same 2:1 layer (Amouric *et al.*, 1978, 1981; Iijima and Buseck, 1978). These images show for all the samples that the polytype is 1*M* with well-ordered stacking (Figure 3). According to Amouric and Olives (1991), 1*M* illite crystals are produced by a dissolution-crystallization mechanism.

Chemistry

Structural formulae of illite-smectite were normalized on the basis of $O_{10}(OH)_2$. The related standard

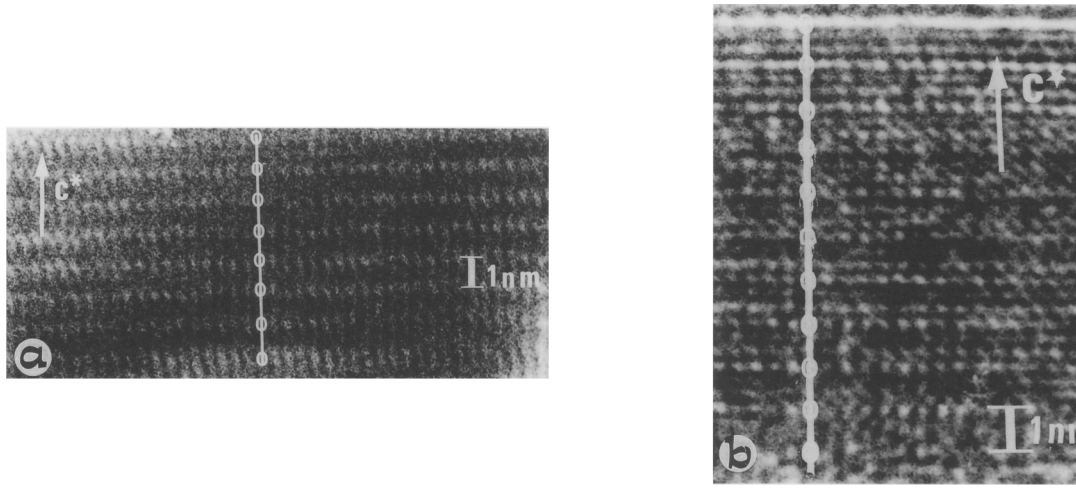

Figure 3. Structure images of illite crystals, from (a) the smectite-rich sample and (b) an illite-rich sample. The illite crystals are of a regular 1*M* polytype. [Image (a) from Amouric and Olives, 1991.]

deviations are 0.06 for Si and Al, 0.04 for Mg and Fe, and 0.02 for Ca and K. On the basis of AEM microanalyses, smectite, illite, and interstratified illite-smectite are dioctahedral. By grouping Fe (considered as Fe^{3+}) with octahedral Al, and Ca with K (Na being neglected), the analyses are illustrated in the pyrophyllite $Si_4Al_2O_{10}(OH)_2$-muscovite $K(Si_3Al)Al_2O_{10}(OH)_2$-celadonite $KSi_4(AlMg)O_{10}(OH)_2$ diagram of Figure 4. Mixed-layer illite-smectite shows a chemical trend from montmorillonite to illite. The chemical reaction involves the fixation of K and (tetrahedral and octahedral) Al in montmorillonite, to produce illite and the emission of H_2O, Si, Mg, and Fe. On the basis of four tetrahedral cations, the number of Fe atoms decreases from 0.08 in the smectite-rich sample to 0.04 in the illite-rich samples and the number of Ca atoms is nearly constant at 0.04. This indicates a chemical modification of the interlayer, tetrahedral, and octahedral cations.

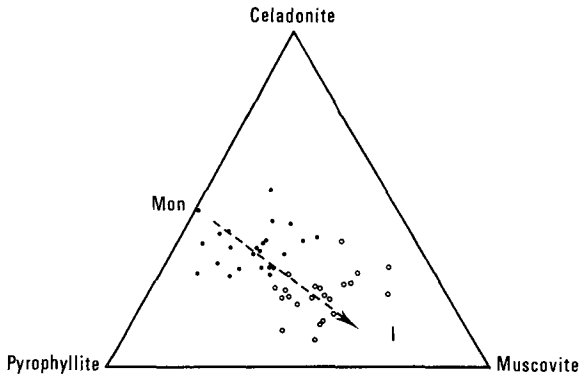

Figure 4. AEM microanalyses of mixed-layer illite-smectite, from the smectite-rich sample (black circles) and the illite-rich samples (open circles) studied. Note the chemical trend from montmorillonite (Mon) to illite (I).

ELECTROSTATIC-ENERGY CALCULATIONS

For a better understanding of the structure and the stability of interstratified illite-smectite, electrostatic-energy calculations were performed to compare the energies of various possible mixed-layer structures with illite and smectite as end-members. For this case, the energy thermodynamic function is adequate because the energy of mixing of the layers is nearly equal to the enthalpy of mixing (where the cell volumes are assumed constant) and to the Gibbs free energy of mixing (because the configurational entropy of mixing vanishes for the perfectly ordered sequences studied). Vibrational aspects were not taken into account. A first approximation to the lattice energy is given by the electrostatic Ewald energy (or Madelung energy). Justification is presented below. The Ewald energies are calculated from the "overlap method" (Olives, 1986a, section 2.4.2), which is presented in the following section. The convergence of this method is rapid, compared to the classical methods of Ewald (1921) or Bertaut (1952).

The overlap method

The electrostatic energy of an ionic crystal in which the ions are considered as point charges was calculated by Madelung (1918) for the special case of cubic crystals, and then by Ewald (1921), who gave a general formula valid for any crystal. Owing to the long-range nature of electrostatic interactions, the electrostatic energy per volume unit (more precisely, the limit of this energy when the crystal becomes infinitely large) depends on the atomic configuration of the surface of the crystal. The Ewald energy represents the minimum of this electrostatic energy per volume unit with respect to all possible atomic configurations of the surface of the crystal (Olives, 1986b, 1987).

Table 1. Interstratified structures corresponding to I'TOT units, TI'TO units, *etc.*, for the ordered layer sequences . . .ISIS. . . and . . .IISIIS. . . (I = illite, S = smectite; I', T, and O, respectively, denote the interlayer, tetrahedral, and octahedral regions). The subscripts I, S, and M, respectively, refer to compositions of illite, smectite, and midway between at 0.5.

Units involved in the interstratification	Interstratified structures for . . .ISIS. . .	Interstratified structures for . . .IISIIS. . .
I'TOT units	. . .$(I'TOT)_I(I'TOT)_S$. . .	. . .$(I'TOT)_I(I'TOT)_I(I'TOT)_S$. . .
TI'TO units	. . .$(TI'TO)_I(TI'TO)_S$. . .	. . .$(TI'TO)_I(TI'TO)_I(TI'TO)_S$. . .
$I'_{0.5}TOTI'_{0.5}$ units	. . .$I'_M(TOT)_II'_M(TOT)_S$. . .	. . .$I'_M(TOT)_II'_I(TOT)_II'_M(TOT)_S$. . .
$T_{0.5}I'TOT_{0.5}$ units	. . .$T_M(I'TO)_IT_M(I'TO)_S$. . .	. . .$T_M(I'TO)_IT_I(I'TO)_IT_M(I'TO)_S$. . .
$O_{0.5}TI'TO_{0.5}$ units	. . .$O_M(TI'T)_IO_M(TI'T)_S$. . .	. . .$O_M(TI'T)_IO_I(TI'T)_IO_M(TI'T)_S$. . .

In the overlap method, the Ewald energy, E, is calculated as $E = E_1 - E_2 + E_3$, in which E_1 is the reciprocal-lattice sum, $E_1 = (1/2\pi V) \sum_{h\neq 0} |F(h)\varphi(h)|^2/h^2$, with

$$F(h) = \sum_u q_u \exp(2\pi i h \cdot u),$$

$$\varphi(h) = 3(\sin\alpha - \alpha\cos\alpha)/\alpha^3, \qquad \alpha = 2\pi R\|h\|;$$

$$E_2 = (3/5R)\sum_u q_u^2;$$

and E_3 is the direct lattice sum,

$$E_3 = (1/2R) \sum_n \sum_u \sum_v q_u q_v \quad (n + u \neq v;\ \|n + u - v\| < 2R)$$

$$\times (1/x - 6/5 + x^2/2 - 3x^3/16 + x^5/160),$$

with

$$x = \|n + u - v\|/R.$$

In these expressions, n denotes the lattice vectors, u or v denotes the positions of the ions of the origin cell $n = 0$, q_u is the charge of the ion at position u, h denotes the reciprocal-lattice vectors, V is the volume of the cell, R is a length parameter of any positive value (E does not depend on R), $i = \sqrt{-1}$, $h \cdot u$ denotes the inner product, and $\|y\|$ denotes the length of any vector y.

As R increases, the number of terms in the finite sum E_3 increases but, at the same time, the series E_1 converges more rapidly. In our case, a very rapid convergence was obtained with a value of R close to the cell dimension, *e.g.*, at $R = 1$ nm.

Smectite and illite

Because the smectite and illite structures are not known accurately, we have used the coordinates from Jenkins and Hartman (1979) as derived from Sidorenko *et al.* (1975) for an Al-rich 1*M* mica for the structure of illite, (dehydrated) smectite, and interstratified illite-smectite. The 1*M* polytype was assumed for the three minerals. The structure relaxation was neglected. Various compositions were used, namely the two compositions of illite, $I_1 = K_{0.75}(Si_{3.6}Al_{0.4})(Al_{1.65}Mg_{0.35})O_{10}(OH)_2$ and $I_2 = K_{0.75}(Si_{3.25}Al_{0.75})Al_2O_{10}(OH)_2$, and the two compositions of (dehydrated) smectite, $S_1 = (Na, K)_{0.35}Si_4(Al_{1.65}Mg_{0.35})O_{10}(OH)_2$ (montmorillonite) and $S_2 = (Na, K)_{0.35}(Si_{3.65}Al_{0.35})Al_2O_{10}(OH)_2$ (beidellite). Formal charges, $q_K = q_{Na} = 1$, $q_{Si} = 4$, $q_{Al} = 3$, $q_{Mg} = 2$, $q_H = 1$, $q_O = -2$, were used with mean charges for the interlayer, tetrahedral, and octahedral cations, *e.g.*, 0.75, $[(3.6 \times 4) + (0.4 \times 3)]/4$, and $[(1.65 \times 3) + (0.35 \times 2)]/2$, respectively, for the above I_1 composition. The Ewald energies of illite I_1, illite I_2, smectite S_1, and smectite S_2 were calculated at −80.5842, −80.1635, −81.9968, and −81.5261 MJ mol^{-1}, respectively (12 oxygen atoms per molecule; 1 MJ = 10^6 J). The uncertainty of these values and the following ones are $<0.5 \times 10^{-4}$ MJ mol^{-1}.

Mixed-layer illite-smectite

Illite and smectite have the same general structure . . .I'TOTI'TOT. . . (TOT layers separated by interlayer regions I'), but the I', T, and O regions are occupied by different cations. A fundamental problem concerning the nature of mixed-layer illite-smectite is the structure of the individual illite and smectite layers. Possibilities include: I'TOT units, TI'TO units, *etc.* Table 1 shows the interstratified structures corresponding to unit layers, for two ordered layer sequences . . .ISIS. . . and . . .IISIIS. . . . In this table, the subscript M indicates a composition midway between illite and smectite at 0.5 and refers to a random mixture of the corresponding cations. Thus, for O_M, with the above I_2 and S_1 compositions, the mean charge, $[3 + (1.65 \times 3 + 0.35 \times 2)/2]/2$, is used for the octahedral cations. Note that, either for the . . .ISIS. . . or for the . . .IISIIS. . . case, the derived structures have the same first-neighbor interactions (oxygen-cation and oxygen-oxygen), although the arrangements differ. Thus, the short-range energies (van der Waals attraction, overlap repulsion) are identical for these structures, and the differences between the lattice energies are only related to the long-range electrostatic energy.

The calculated Ewald energies of the preceding mixed-layer structures are given in Table 2 for . . .ISIS. . . and in Table 3 for . . .IISIIS. . . , for the various compositions used. For all cases, the results indicate that the more stable interstratification structure (minimum energy) is based on $O_{0.5}TI'TO_{0.5}$ units.

Table 2. Calculated Ewald energies of the mixed-layer structures corresponding to I'TOT units, TI'TO units, *etc.* (see Table 1), for the ordered layer sequence . . .ISIS. . .. The last column gives the Ewald energy of the two-phases illite + smectite assemblage with the same composition (*i.e.*, energy of illite + energy of smectite). Various compositions of illite (I_1, I_2) and smectite (S_1, S_2) were used (see text). Values are in MJ mol^{-1} = 10^6 J mol^{-1} and refer to 24 oxygen atoms per molecule. The more stable interstratification structure (minimum energy) is based on $O_{0.5}TI'TO_{0.5}$ units. The energy of the mixed-layer . . .ISIS. . . (with $O_{0.5}TI'TO_{0.5}$ units) is close to the corresponding energy of the two-phases illite + smectite assemblage.

Compositions	Interstratified sequence . . .ISIS. . .					Two-phase illite + smectite assemblage
	I'TOT units	TI'TO units	$I'_{0.5}TOTI'_{0.5}$ units	$T_{0.5}I'TOT_{0.5}$ units	$O_{0.5}TI'TO_{0.5}$ units	
I_1S_1	−162.5088	−162.5809	−162.5381	−162.5558	−162.5809	−162.5809
I_1S_2	−162.0361	−162.0533	−162.0654	−162.0449	−162.0867	−162.1103
I_2S_1	−162.0903	−162.1031	−162.1196	−162.1350	−162.1365	−162.1602
I_2S_2	−161.6175	−161.6896	−161.6468	−161.6645	−161.6896	−161.6896

Moreover, this model corresponds to the minimum energy in comparison to the other models based on $O_xTI'TO_{1-x}$, $I'_xTOTI'_{1-x}$, or $T_xI'TOT_{1-x}$ units ($0 \leq x \leq 1$). This result indicates that the layers involved in the interstratification are probably $O_{0.5}TI'TO_{0.5}$ (Olives and Amouric, 1994a, 1994b). When the octahedral compositions of illite and smectite are identical, *i.e.*, for I_1S_1 and I_2S_2, note that the interstratification structure based on $O_{0.5}TI'TO_{0.5}$ units coincides with that based on TI'TO units. The interstratification may then be described as the superposition of illitic or smectitic TI'T units, separated by octahedral sheets of M, I, or S composition (for the respective cases of IS, II, or SS adjacent layers). Figure 5 illustrates an example of the . . .ISIS. . . interstratification. The lattice-energy calculations lead to a polar model for TOT layers (with two tetrahedral sheets of different compositions; see *e.g.*, Güven, 1991). Indeed, the precise arrangement is $T_IO_MT_S$ for the case of IS adjacent layers. Such a polar model (first proposed by Sudo *et al.*, 1962) is in agreement with expandability measurements, XRD analysis, and HRTEM imaging (*e.g.*, Reynolds, 1980; Jiang *et al.*, 1990; Veblen *et al.*, 1990), and is supported by NMR spectroscopy (Barron *et al.*, 1985; Altaner *et al.*, 1988; Jakobsen *et al.*, 1995). On the basis of these results, Altaner and Ylagan (1997) also favored the polar model and assumed this model to compare the mechanisms for smectite illitization.

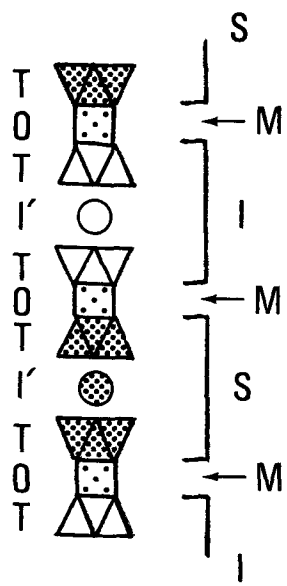

Figure 5. Structure of the ordered mixed-layer illite-smectite . . .ISIS. . . as determined by the minimization of the lattice energy. The corresponding arrangement is . . . $O_M(TI'T)_IO_M(TI'T)_S$ . . . (I', T, O = interlayer, tetrahedral, and octahedral regions, respectively; I, S, M = compositions of illite, smectite, and midway between at 0.5, respectively).

Furthermore, the energies obtained for the mixed-layers . . .ISIS. . . and . . .IISIIS. . . (with $O_{0.5}TI'TO_{0.5}$ units) are close to the corresponding energies of the two-phase assemblage of illite + smectite (Tables 2 and 3). Thus, the energy of mixing of the two types of layers is nearly equal to zero. When the octahedral compositions of illite and smectite are identical, *i.e.*, for I_1S_1 and I_2S_2, note that the energy of the mixed-layer is equal to that of the two-phase assemblage of illite + smectite. A similar result was obtained for interstratified biotite-chlorite (Olives, 1985, 1986a). The stability of interlayered illite-smectite is then similar to the stability of an assemblage containing discrete illite and smectite. This result may explain the coexistence of illite, smectite, and interstratified illite-smectite, which was observed in our smectite-rich sample (Amouric and Olives, 1991; also *e.g.*, Dong *et al.*, 1997).

Summary of assumptions

The electrostatic Ewald energy was considered as a first approximation to the lattice energy. Ewald energies were calculated from the overlap method (Olives, 1986a, section 2.4.2) which provides rapid convergence. Formal charges were used. Random distribution of cations in each octahedral, tetrahedral, or interlayer region was assumed. Identical coordinates were used for the structure of illite, (dehydrated) smectite, and interstratified illite-smectite (1*M* polytype was assumed for the three minerals). Structure relaxation was neglected. Two compositions of illite (I_1, I_2) and two compositions of smectite (S_1, S_2) were used.

Table 3. Calculated Ewald energies of the mixed-layer structures corresponding to I'TOT units, TI'TO units, *etc.* (see Table 1), for the ordered layer sequence . . .IISIIS. . . The last column gives the Ewald energy of the two-phase assemblage of illite + smectite with the same composition (*i.e.*, 2 × energy of illite + energy of smectite). Various compositions of illite (I_1, I_2) and smectite (S_1, S_2) were used (see text). Values are in MJ mol^{-1} = 10^6 J mol^{-1} and refer to 36 oxygen atoms per molecule. The more stable interstratification structure (minimum energy) is based on $O_{0.5}TI'TO_{0.5}$ units. The energy of the mixed-layer . . .IISIIS. . .(with $O_{0.5}TI'TO_{0.5}$ units) is close to the corresponding energy of the two-phases illite + smectite assemblage.

Compositions	Interstratified sequence . . .IISIIS. . .					Two-phase illite + smectite assemblage
	I'TOT units	TI'TO units	$I'_{0.5}TOTI'_{0.5}$ units	$T_{0.5}I'TOT_{0.5}$ units	$O_{0.5}TI'TO_{0.5}$ units	
$I_1I_1S_1$	−243.0682	−243.1651	−243.1223	−243.1337	−243.1651	−243.1651
$I_1I_1S_2$	−242.5954	−242.6184	−242.6495	−242.6072	−242.6708	−242.6944
$I_2I_2S_1$	−242.2289	−242.2476	−242.2830	−242.2984	−242.3000	−242.3237
$I_2I_2S_2$	−241.7561	−241.8531	−241.8103	−241.8217	−241.8531	−241.8531

Consequences for the smectite-to-illite solid-state mechanism

In Amouric and Olives (1991), two illitization mechanisms were detected on the basis of HRTEM observations: (1) dissolution of smectite and crystallization of illite, which produces 1*M* illite crystals, and (2) solid-state transformation of one smectite layer to one illite layer, which leads to mixed-layer illite-smectite. This latter mechanism was also supported by the HRTEM study of Murakami *et al.* (1993). The term "solid-state" is used here in a broad sense, because mass transport is obviously involved in such a transition. Thus, the transformation occurs within a solid, at the unit-cell scale, at the boundary of the newly developing layer and the reaction is probably facilitated by the presence of water. The major part of the preexisting solid is preserved (*e.g.*, Veblen and Buseck, 1980; Olives *et al.*, 1983; Eggleton and Banfield, 1985; Amouric and Olives, 1998). The interstratification determined by the above calculations has important consequences for this transformation: the mechanism probably consists of a lateral transformation of an $O_{0.5}TI'TO_{0.5}$ unit of smectite into the same unit of illite. The reaction most probably begins at the interlayer, I', because of its high ion and water-exchange capacity, and propagates to the two adjacent $TO_{0.5}$ units. The reaction then laterally runs along the layer so that an $O_{0.5}TI'TO_{0.5}$ unit of smectite is progressively transformed into the same corresponding unit of illite.

ACKNOWLEDGMENTS

We thank A. Inoue for providing the samples studied. We also acknowledge the helpful comments of S. Guggenheim, P. Heaney, R. Cygan, and H. Dong.

REFERENCES

Ahn, J.H. and Peacor, D.R. (1989) Illite/smectite from Gulf Coast shales: A reappraisal of transmission electron microscope images. *Clays and Clay Minerals,* **37,** 542–546.

Altaner, S.P. and Ylagan, R.F. (1997) Comparison of structural models of mixed-layer illite/smectite and reaction mechanisms of smectite illitization. *Clays and Clay Minerals,* **45,** 517–533.

Altaner, S.P., Weiss, C.A., and Kirkpatrick, R.J. (1988) Evidence from ^{29}Si NMR for the structure of mixed-layer illite/smectite clay minerals. *Nature,* **331,** 699–702.

Amouric, M. and Olives, J. (1991) Illitization of smectite as seen by high-resolution transmission electron microscopy. *European Journal of Mineralogy,* **3,** 831–835.

Amouric, M. and Olives, J. (1998) Transformation mechanisms and interstratification in conversion of smectite to kaolinite: An HRTEM study. *Clays and Clay Minerals,* **46,** 521–527.

Amouric, M., Baronnet, A., and Finck, C. (1978) Polytypisme et désordre dans les micas dioctaédriques synthétiques; étude par imagerie de réseau. *Materials Research Bulletin,* **13,** 627–634.

Amouric, M., Mercuriot, G., and Baronnet, A. (1981) On computed and observed HRTEM images of perfect mica polytypes. *Bulletin de Minéralogie,* **104,** 298–313.

Barron, P.F., Slade, P., and Frost, R.L. (1985) Ordering of aluminium in tetrahedral sites in mixed-layer 2:1 phyllosilicates by solid-state high-resolution NMR. *Journal of Physical Chemistry,* **89,** 3880–3885.

Bertaut, F. (1952) L'énergie électrostatique de réseaux ioniques. *Le Journal de Physique et le Radium,* **13,** 499–505.

Buatier, M.D., Peacor, D.R., and O'Neil, J.R. (1992) Smectite-illite transition in Barbados accretionary wedge sediments: TEM and AEM evidence for dissolution/crystallization at low temperature. *Clays and Clay Minerals,* **40,** 65–80.

Cliff, G. and Lorimer, G.W. (1975) The quantitative analysis of thin specimens. *Journal of Microscopy,* **103,** 203–207.

Dong, H., Peacor, D.R., and Freed, R.L. (1997) Phase relations among smectite, R1 illite-smectite, and illite. *American Mineralogist,* **82,** 379–391.

Eggleton, R.A. and Banfield, J.F. (1985) The alteration of granitic biotite to chlorite. *American Mineralogist,* **70,** 902–910.

Ewald, P.P. (1921) Die berechnung optischer und elektrostatischer gitterpotentiale. *Annalen der Physik,* **64,** 253–287.

Guthrie, G.D. and Veblen, D.R. (1989) High-resolution transmission electron microscopy of mixed-layer illite/smectite: Computer simulations. *Clays and Clay Minerals,* **37,** 1–11.

Guthrie, G.D. and Veblen, D.R. (1990) Interpreting one-dimensional high-resolution transmission electron micrographs of sheet silicates by computer simulations. *American Mineralogist,* **75,** 276–288.

Güven, N. (1991) On the definition of illite/smectite mixed-layer. *Clays and Clay Minerals,* **39,** 661–662.

Huggett, J.M. (1995) Formation of authigenic illite in palaeocene mudrocks from the central North Sea: A study by high resolution electron microscopy. *Clays and Clay Minerals,* **43,** 682–692.

Iijima, S. and Buseck, P.R. (1978) Experimental study of disordered mica structures by high-resolution electron microscopy. *Acta Crystallographica A,* **34,** 709–719.

Inoue, A. and Utada, M. (1983) Further investigations of a conversion series of dioctahedral mica/smectites in the

Shinzan hydrothermal alteration area, northeast Japan. *Clays and Clay Minerals,* **31,** 401–412.

Inoue, A., Kohyama, N., Kitagawa, R., and Watanabe, T. (1987) Chemical and morphological evidence for the conversion of smectite to illite. *Clays and Clay Minerals,* **35,** 111–120.

Jakobsen, H.J., Nielsen, N.C., and Lindgreen, H. (1995) Sequences of charged sheets in rectorite. *American Mineralogist,* **80,** 247–252.

Jenkins, H.D.B. and Hartman, P. (1979) A new approach to the calculation of electrostatic energy relations in minerals: The dioctahedral and trioctahedral phyllosilicates. *Philosophical Transactions of the Royal Society of London A,* **293,** 169–208.

Jiang, W.T., Peacor, D.R., Merriman, R.J., and Roberts, B. (1990) Transmission and analytical electron microscopic study of mixed-layer illite/smectite formed as an apparent replacement product of diagenetic illite. *Clays and Clay Minerals,* **38,** 449–468.

Madelung, E. (1918) Das elektrische feld in systemen von regelmäßig angeordneten punktladungen. *Physikalische Zeitschrift,* **19,** 524–532.

Murakami, T., Sato, T., and Watanabe, T. (1993) Microstructure of interstratified illite/smectite at 123K: A new method for HRTEM examination. *American Mineralogist,* **78,** 465–468.

Olives, J. (1985) Biotites and chlorites as interlayered biotite-chlorite crystals. *Bulletin de Minéralogie,* **108,** 635–641.

Olives, J. (1986a) The Ewald energies of complex crystals: The "biochlorites". *Acta Crystallographica A,* **42,** 340–344.

Olives, J. (1986b) The electrostatic lattice energy. *Physica Status Solidi (b),* **138,** 457–464.

Olives, J. (1987) The electrostatic energy of a lattice of point charges. *Annales de l'Institut Henri Poincaré, Physique Théorique,* **47,** 125–184.

Olives, J. and Amouric, M. (1994a) Transformation of smectite into illite and illite-smectite interstratification: HRTEM observations and lattice energies calculations. In *Electron Microscopy 1994, Proceedings of the 13th International Congress on Electron Microscopy, Volume 2B,* B. Jouffrey and C. Colliex, eds., Les Editions de Physique, Paris, 1281–1282.

Olives, J. and Amouric, M. (1994b) Illite-smectite interstratified minerals in the smectite-to-illite transition. In *Abstracts of the 16th General Meeting of the International Mineralogical Association,* S. Merlino, ed., Societa Italiana di Mineralogia e Petrologia, Pisa, 309–310.

Olives, J., Amouric, M., de Fouquet, C., and Baronnet, A. (1983) Interlayering and interlayer slip in biotite as seen by HRTEM. *American Mineralogist,* **68,** 754–758.

Reynolds, R.C. (1980) Interstratified clay minerals. In *Crystal Structures of Clay Minerals and Their X-ray Identification,* G.W. Brindley and G. Brown, eds., Mineralogical Society, London, 249–303.

Reynolds, R.C. (1992) X-ray diffraction studies of illite/smectite from rocks, <1 μm randomly oriented powders, and <1 μm oriented powder aggregates: The absence of laboratory-induced artifacts. *Clays and Clay Minerals,* **40,** 387–396.

Sidorenko, O.V., Zvyagin, B.B., and Soboleva, S.V. (1975) Crystal structure refinement for 1M dioctahedral mica. *Soviet Physics, Crystallography,* **20,** 332–335.

Środoń, J. (1984) X-ray powder diffraction identification of illitic materials. *Clays and Clay Minerals,* **32,** 337–349.

Sudo, T., Hayasi, H., and Shimoda, S. (1962) Mineralogical problems of intermediate clay minerals. In *Proceedings of the 9th National Conference on Clays and Clay Minerals, Lafayette, Indiana, 1960,* A. Swineford, ed., Pergamon Press, New York, 378–388.

Veblen, D.R. and Buseck, P.R. (1980) Microstructures and reaction mechanisms in biopyriboles. *American Mineralogist,* **65,** 599–623.

Veblen, D.R., Guthrie, G.D., Livi, K.J.T., and Reynolds, R.C. (1990) High-resolution transmission electron microscopy and electron diffraction of mixed-layer illite/smectite: Experimental results. *Clays and Clay Minerals,* **38,** 1–13.

E-mail of corresponding author: olives@crmc2.univ-mrs.fr

(Received 11 December 1998; accepted 10 December 1999; Ms. 98-138; A.E. Peter J. Heaney)